Design and synthesis of 2-((1H-indol-3-yl)thio)-N-phenyl-acetamides as novel dual inhibitors of respiratory syncytial virus and influenza virus A

Guo-Ning Zhang, Qiang Li, Jianyuan Zhao, Xuandi Zhang, Zhuxin Xu, Yujia Wang, Yuanhui Fu, Qi Shan, Yanpeng Zheng, Juxian Wang, Mei Zhu, Ziqiang Li, Shan Cen, Jinsheng He, Yucheng Wang

PII: S0223-5234(19)31013-X

DOI: https://doi.org/10.1016/j.ejmech.2019.111861

Reference: EJMECH 111861

To appear in: *European Journal of Medicinal Chemistry*

Received Date: 5 February 2019

Revised Date: 15 October 2019

Accepted Date: 5 November 2019

Please cite this article as: G.-N. Zhang, Q. Li, J. Zhao, X. Zhang, Z. Xu, Y. Wang, Y. Fu, Q. Shan, Y. Zheng, J. Wang, M. Zhu, Z. Li, S. Cen, J. He, Y. Wang, Design and synthesis of 2-((1H-indol-3-yl)thio)-N-phenyl-acetamides as novel dual inhibitors of respiratory syncytial virus and influenza virus A, *European Journal of Medicinal Chemistry* (2019), doi: https://doi.org/10.1016/j.ejmech.2019.111861.

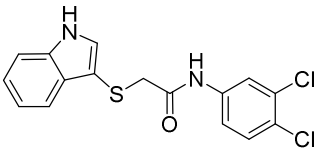

1

Inhibition of RSV at 50μM: 77.14%
Cell Viability at 50μM: 81.77%

lead optimazation

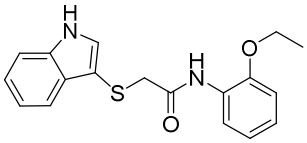

2

Inhibition of RSV at 50μM: 83.24%
Cell Viability at 50μM: 65.21%

RSV and IAV dual inhibitors	IC_{50} (μM)	Safety Index	virus
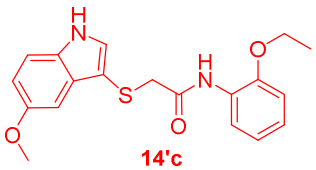 **14'c**	4.82±0.99	379.25	RSV
	1.27±0.07	>79.37	IAV
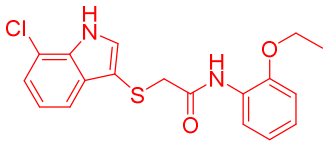 **14'e**	4.46±0.28	58.81	RSV
	1.75±0.96	>57.47	IAV
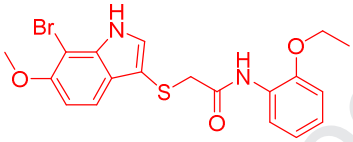 **14'i**	2.92±0.77	3.30	RSV
	1.90±0.05	>52.63	IAV

Short communication

Design and synthesis of 2-((1H-indol-3-yl)thio)-N-phenyl-acetamides as novel dual inhibitors of respiratory syncytial virus and influenza virus A

Guo-Ning Zhang[a,#], Qiang Li[a, #], Jianyuan Zhao[a], Xuandi Zhang[a, b], Zhuxin Xu[c], Yujia Wang[a], Yuanhui Fu[c], Qi Shan[a], Yanpeng Zheng[c], Juxian Wang[a], Mei Zhu[a], Ziqiang Li[b], Shan Cen[a*], Jinsheng He[c*], Yucheng Wang[a*]

[a.] *Institute of Medicinal Biotechnology, Chinese Academy of Medical Science and Peking Union Medical College, Beijing 100050, China*；

[b.] *School of Pharmacy, Jinzhou Medical University, Jinzhou, Liaoning 121001, China*

[c.] *College of Life Sciences and Bioengineering, Beijing Jiaotong University, Beijing 100044, China*

* Corresponding author.

E-mail address: shancen@imb.pumc.edu.cn (S. Cen); jshhe@bjtu.edu.cn (J. He); wangyucheng@imb.pumc.edu.cn (Y. Wang).

[#] Both authors contributed equally to this work.

Abbreviations

Respiratory syncytial virus, RSV; influenza A virus, IAV; human parainfluenza viruses, HPIV; human metapneumoviruses, HMPV; acute respiratory infections, ARIs; plaque-forming units, pfu; Gaussia luciferase, Gluc; Relative fluorescence units, RFU; Madin-Darby Canine Kidney, MDCK; 1-Ethyl-3-(3-Dimethylaminopropyl) Carbodiimide, EDC; Hexafluorophosphate Azabenzotriazole Tetramethyl Uronium, HATU.

ABSTRACT

Respiratory syncytial virus (RSV) and influenza A virus (IAV) are two of the most common viruses that cause substantial morbidity and mortality in infants, young children, elderly persons, and immunocompromised individuals worldwide. Currently, there are no licensed vaccines or selective antiviral drugs against RSV infections and most IAV strains become resistant to clinical anti-influenza drug. Here, we described the discovery of a series of 2-((1H-indol-3-yl)thio)-N-phenyl-acetamide as novel and potent RSV and IAV dual inhibitors. Thirty-five derivatives were designed, prepared, and evaluated for their anti-RSV and anti-IAV activities. Among the tested compounds, **14'c**, **14'e**, **14'f**, **14'h**, and **14'i** exhibited excellent activity against both RSV and IAV, which showed low micromolar to sub-micromolar EC_{50} values. Further, compounds **14'c** and **14'e** were identified as the most promising dual inhibitors with lesser cytotoxicity than the clinical drug, ribavirin. These findings may contribute to the development of a lead compound for the treatment of RSV and/or IAV infections.

Keywords: 2-((1H-indol-3-yl)thio)-N-phenyl-acetamide; respiratory syncytial virus; influenza A virus; dual inhibitors

1. Introduction

Pneumonia is the leading cause of death for children under 5 years-old and accounts for approximately 15% of total deaths in this age spectrum worldwide [1-3]. With the availability of vaccines, the infection rate of *Streptococcus pneumoniae* (pneumococcus) and *Haemophilus influenzae* type b has decreased, and viruses have become the main pathogen of acute respiratory infections including pneumonia [4]. Respiratory viruses are considered to be major contributors to acute respiratory infections in children and are associated with almost 60% of acute respiratory infections (ARIs) [4]. The most frequently reported viruses include respiratory syncytial virus (RSV), Influenza A and B viruses (IAV, IBV), human rhinovirus (HRV), parainfluenza viruses (PIVs), and adenovirus (ADV), which are responsible for most episodes of ARIs in children.

RSV is a negative stranded non-segmented RNA virus of the pneumovirus family. To add, it is the most common respiratory virus in infants, young children, elderly persons, and immunocompromised persons worldwide [5]. RSV is the leading cause of hospitalization for infants, especially those born premature or with chronic lung or heart disease [6, 7]. Almost all infants are infected at least once by RSV by the age of three, and severe lower respiratory tract infection by RSV is estimated to be the cause of ~3.4 million hospitalizations and ~200,000 deaths worldwide [8]. RSV infection has also been associated with a greater risk of long-term development of recurrent wheezing and asthma in children [9]. Despite the substantial economic impact and the

medical needs associated with severe viral infection, neither vaccines nor a specific antiviral therapy is currently available for RSV infection [10]. Instead, treatment therapy is limited to the non-specific antiviral drug, ribavirin (**Figure 1**), which is teratogenic and displays limited efficacy. The monoclonal antibody, palivizumab, has demonstrated effectiveness as prophylaxis in infants who are premature or have underlying comorbidities [11]. To add, some candidates, such as lumicitabine (ALS-8176), presatovir (GS-5806), PC-786, JNJ-678, AK-0529, and TMC353121 (**Figure 1**) are in clinical development as anti RSVs [12-17]. In RSV-infected hospitalized children under two years-old, higher viral loads on the third day after hospitalization have been linked to an increased requirement for intensive care and progression to respiratory failure [18]. This result suggests that early and efficacious therapeutics given to hospitalized children may improve downstream morbidity and reduce immunopathology therapeutics.

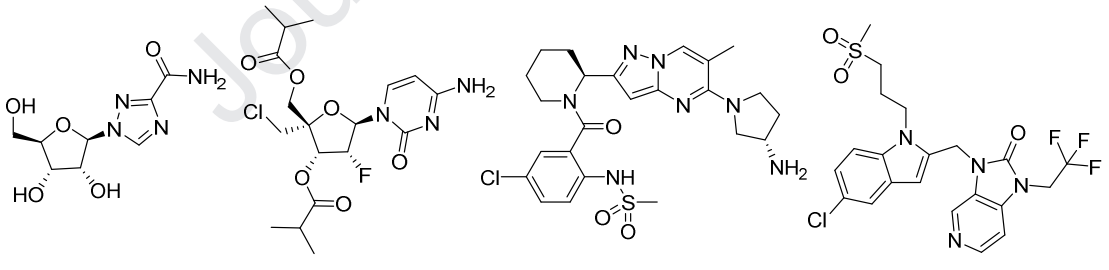

ribavirin ALS-8176 GS-5806 JNJ-678

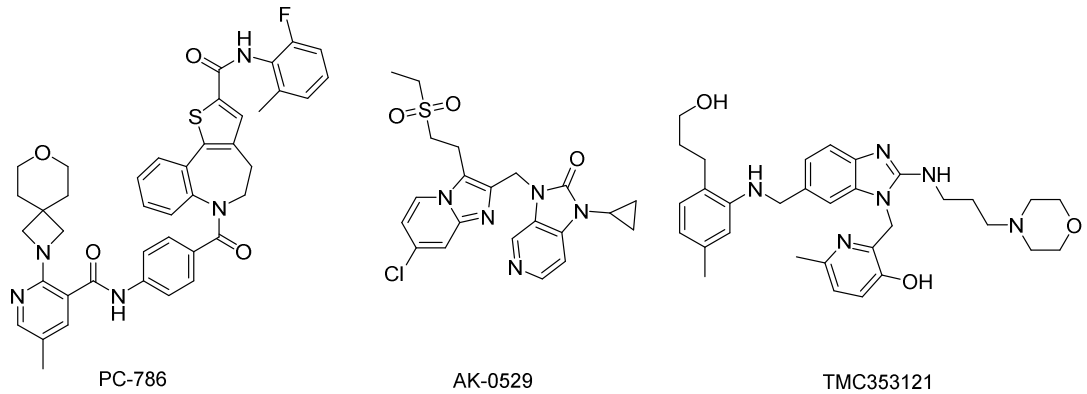

PC-786 AK-0529 TMC353121

Figure 1 Structure of ribavirin, a non-specific anti-viral drug, and candidates in anti-RSV clinical development.

Influenza A virus (IAV) is a negative-stranded segmented RNA virus. IAV infection is one of the major causes of morbidity and mortality due to respiratory disease, and outbreaks of infection sometimes occur in worldwide epidemics. Influenza is estimated to be responsible for 291,000 to 646,000 deaths worldwide [19]. To add, IAV is responsible for most cases of epidemic influenza [20]. Infrequently, novel or reemerging strains of IAV have caused rapid and severe global pandemics, resulting in millions of fatalities. Influenza B virus (IBV) almost exclusively infects humans and is less common than IAV due to its lower genetic diversity. A degree of immunity to IBV is usually acquired at an early age. IAV is often associated with more-severe symptoms, morbidity, and mortality due to a greater genetic diversity typified by chromosomal reassortment between human and avian viruses [21]. Currently, there are only two main classes of antiviral drugs against influenza [22]: M2 ion channel inhibitors, also called adamantanes (amantadine and rimantadine); and neuraminidase inhibitors (oseltamivir and zanamivir) (**Figure 2**), to combat the spread of influenza A. However, most of the influenza A strains have become resistant to adamantanes, and strains resistant to oseltamivir and zanamivir have been reported [23, 24]. An urgent need therefore exists to discover and develop new anti-influenza antivirals.

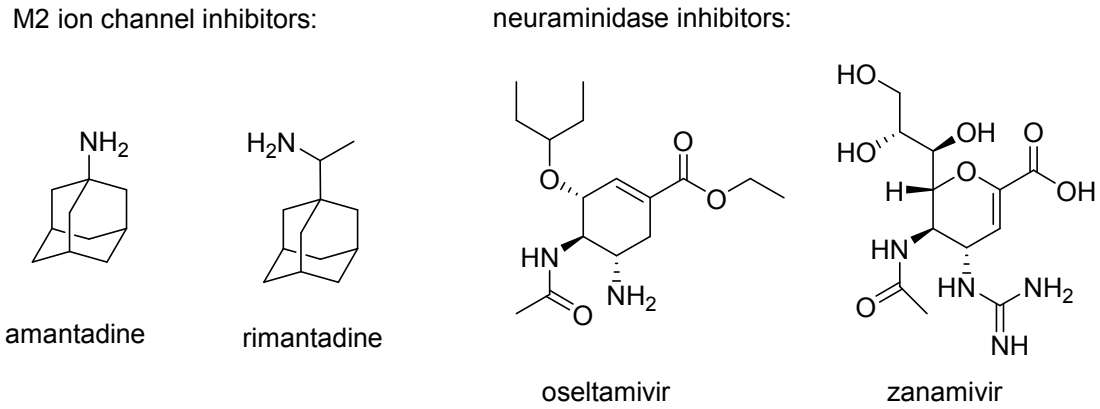

Figure 2 Antiviral drugs against IAV in the clinic.

Patients infected with either influenza virus or RSV can present similar early symptoms [25, 26]; however, the course of therapy and choice of antiviral agent differ for both viruses [21]. The lack of a reliable and fast bedside test to rapidly confirm the viral etiology makes it impossible to perform early administration of antiviral agent, which is an important step toward reducing drug use, especially in hospitalized children. Alternatively, discovering new active chemical entities against RSV and IAV is a simple and efficient strategy for rapid treatment of respiratory infections.

In this work, we initially identified 29 compounds as potent RSV inhibitors using an rRSV-mGFP high-throughput screening assay. After considering toxicity, druggability, and feasibility of the synthesis of these compounds, compounds **1** and **2** were selected as candidates for further optimization (**Figure 3**). These compounds showed moderate to high inhibition (77.14% and 83.24% for **1** and **2**, respectively) in a fluorescence-based assay with little or no toxicity to HEp-2 cells at 50 μM.

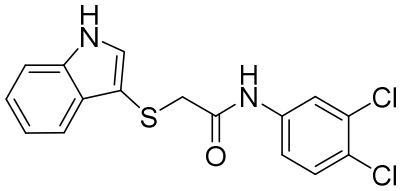

1

Inhibition ratio at 50μM: 77.14%
Cell Viability at 50μM: 81.77%

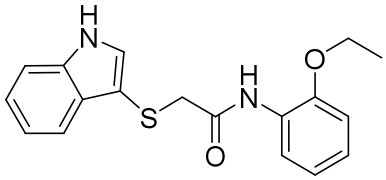

2

Inhibition ratio at 50μM: 83.24%
Cell Viability at 50μM: 65.21%

Figure 3 RSV inhibitors **1** and **2** identified on rRSV-mGFP high-throughput screening platform.

As these two candidates share the common scaffold of 2-((1H-indol-3-yl)thio) acetamide, we believe this fragment is crucial for RSV inhibition and thus, intend to introduce different substituent groups to increase their anti-viral potency. Firstly, a methyl group was introduced to the nitrogen-atoms of indole and a series of derivatives from compound **1** was designed and synthesized. Thereafter, thioethers were oxidized to sulfoxide and sulfone to yield 2 additional series of derivatives. Finally, methoxy-, chlorine atoms, or nitrogen atom was successfully introduced to the benzene ring in indole. These compounds were evaluated for their anti-RSV and anti-IAV activity. Encouragingly, these compounds depicted excellent to moderate activity toward these two viruses, with compounds **14'c**, **14'e**, **14'f**, **14'h**, and **14'i** exhibiting excellent activity and low micromolar to sub-micromolar EC_{50} values. Among the compounds, **14'c** and **14'e**, and **14'f** and **14'i** were identified as the most promising dual inhibitors with lower cytotoxicity than the clinical drug, ribavirin.

2. Materials and methods

2.1. Experimental chemistry

Reagents were purchased from commercial suppliers and used without further

purification, unless otherwise noted. NMR spectra were recorded on Bruker Avance 400 MHz (^{1}H at 400 MHz) and 500 MHz (^{1}H at 500 MHz, ^{13}C at 125 MHz) spectrometer. Chemical shift values are given in ppm with reference to the internal standard, TMS (tetramethylsilane). The peak patterns are indicated as follows: s, singlet; d, doublet; t, triplet; q, quadruplet; m, multiple and dd, doublet of doublets. Coupling constants (*J*) are reported in hertz (Hz). LC-MS data were recorded on Agilent HPLC/MCD instrument. Silica gel column chromatography was performed over silica gel 200-300 mesh, and the eluent was a mixture of ethyl acetate and petroleum ether, or a mixture of methanol and dichloromethane.

2.2. Inhibitor design and synthesis

The structure of 2-((1H-indol-3-yl)thio) acetamide is considered to be a crucial moiety for the RSV inhibition effect, thus methyl-, methoxy-, chlorine or nitrogen atom was subsequently introduced to indole ring in this research.

The target products were synthesized mainly by two routes. In the first route (**Scheme 1**), the N-methyl substituted derivatives was obtained by the coupling of different anilines and 2-((1-methyl-1H-indol-3-yl)thio)acetic acid, which was prepared by the substitution of N-methyl indole in situ. The sulfur atom at position 2 of the indole ring can be oxidized to sulfoxide and sulfone by meta-chloroperoxybenzoic acid.

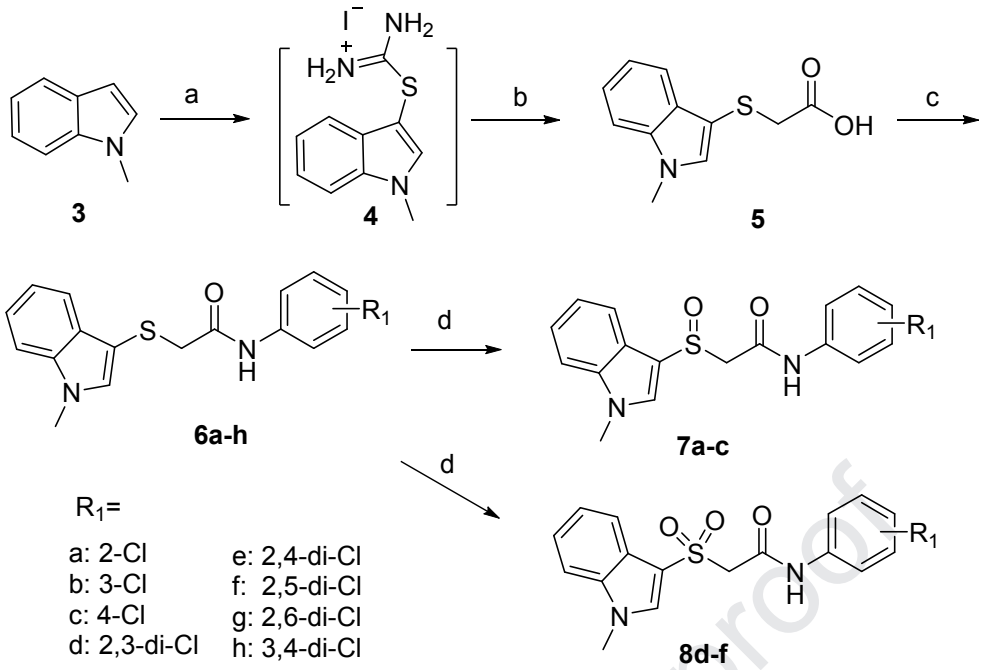

Scheme 1 Reagents and conditions: a). Thiourea, I_2, KI, EtOH/H_2O, 35-40^oC; b). Bromoacetic acid, NaOH, $NH_2NH_2 \cdot H_2O$, 100 ^oC, then 10% HCl; c). substituted aniline, HATU, DIEA, dichloromethane; d). m-CPBA (1 equivalent for 7 series and 2 equivalents for 8 series), dichloromethane.

All other derivatives were obtained using a second route (**Scheme 2**). Commercially-available anilines were acylated with bromoacetyl bromide to yield the corresponding 2-bromo-N-(substituted phenyl) acetamides, which can be converted to sodium S-(2-oxo-2-(phenylamino)ethyl) sulfurothioates using sodium thiosulfate. Subsequently, the sodium sulfurothioates were reacted with substituted indole to yield the target products.

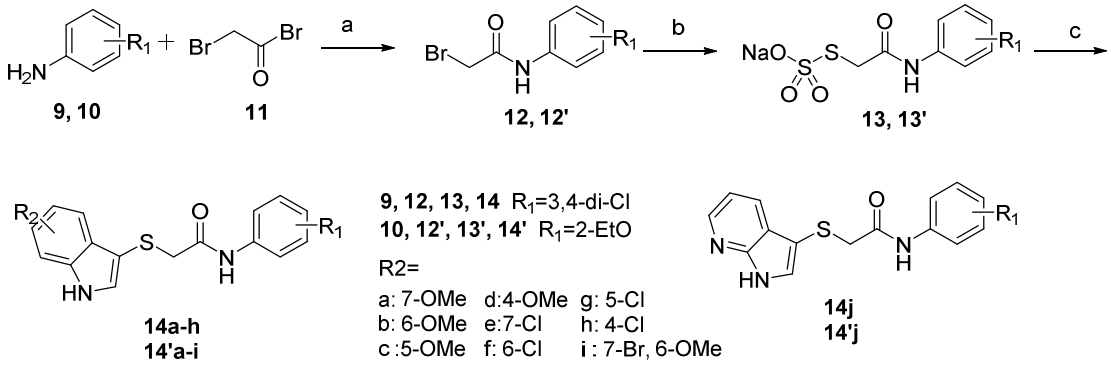

Scheme 2 Reagents and conditions: a). Et_3N, Dichloromethane, 0 ^oC; b). $Na_2S_2O_3 \cdot 5H_2O$, MeOH: H_2O=3:1(v/v), 60 ^oC; c. Substituted indole or azaindole, iodine, DMSO, 60 ^oC

Details regarding the syntheses and characterizations of the compounds can be found in the Supplementary data.

2.3 Viruses and cells

Green Fluorescent Protein expressing recombinant RSV (RSV-mGFP; kindly provided by Prof. Jean-Francois Eleouet, Unite de Virologie et Immunologie Moleculaires (UR892), INRA, Jouy-en-Josas, France) and wild type subgroup A RSV Long strain (*wt*RSV, kindly provided by Prof. Y. Qian, Capital Institute of Pediatrics, Beijing, China) were propagated in HEp-2 cells (ATCC, Rockefeller, MD, USA) in DMEM (Gibco BRL, Gaithersburg, MD, USA) supplemented with 2% fetal bovine serum (FBS, Hyclone, Logan, UT, USA), L-glutamine (2 mmol/L), penicillin G (40 U/ml), streptomycin (100 μg/ml), and 0.2% sodium bicarbonate. RSV-mGFP and *wt*RSV were purified by sucrose ultracentrifugation, titrated for infectivity by immunoplaque assay, and expressed as plaque-forming units (pfu) per ml. HEK293T-Gluc cells were generated by transfection of plasmid DNA pLenti6-Gluc

constitutively expressing the negative-strand RNA of Gaussia luciferase (Gluc) gene, that is converted into the positive strand upon IAV infection, and expresses the Gluc enzyme [27].

2.4 Cytotoxicity assay

Method 1 (for data in Table 1):

All compounds were individually subjected to cytotoxicity assay with MTS method. HEp-2 cells were plated in 96-well plates, and infected with virus alone or together with the test compound after 24 h. Following incubation for 48 h, 20 μl of 2 mg/ml MTS (Promega, Madison, WI, USA) was added to 96-well plates, and cells were further incubated for 3 h at 37 °C in a 5% CO_2 incubator. After shaking the plate for 10 s, absorbance was measured with a microplate reader (Tecan, Mannedorf, Switzerland) at a wavelength of 490 nm. Cells in the mock-treated control were left uninfected by virus or infected but untreated with the test compound. Cell activity was set as 100%.

Method 2 (for data in Table 2):

Cell viability was evaluated by cell counting kit-8 (CCK-8) assay. Briefly, 293T cells were cultured in a 96-well plate and incubated with compounds. Six concentrations of each compound, ranging from 12.5 μM to 200 μM, were used to treat cells for 48 h. Cells cultured in DMSO only were used as the control. After a 48-h incubation, 10 μL CCK-8 solution was added to each well and incubated for an additional 1 h at 37 °C. Optical density (OD) of each well at 450 nm was recorded on a Microplate Reader

(Thermo, Varioskan Flash).

2.5 RSV replication assay

The compounds tested was dissolved in DMSO as a solution of 100mM and diluted to the concentration indicated. HEp-2 cells in different concentrations were plated in 96-well flat bottom black plates. After 24 h, HEp-2 cells were infected with 3-fold serially-diluted viral inocula starting from 3×10^4 pfu/well. Relative fluorescence units (RFU) were measured using multi-mode microplate reader (Molecular Devices, Silicon Valley, USA) with excitation wavelength of 479 nm and emission wavelengths of 517 nm at 24 h, 48 h, and 72 h post-infection. Non-infected HEp-2 cells were severed as background levels of the fluorescence.

2.6. IAV replication assay

HEK293T-Gluc and MDCK cells were incubated with IAV A/WSN/33 (H1N1) (or H3N2) for 1 h at room temperature, and then cultured in fresh DMEM for 24 h at 37 °C. Gluc activity in culture medium was measured as described previously [28]. Briefly, coelenterazine-h (16.7 μM in PBS) was equilibrated for 30 min in the dark at room temperature. Thereafter, cell culture supernatants were added to the wells in white and opaque 96-well plates, followed by automated injection of 60 μl of coelenterazine-h per well. The 0.5-s photon counts were acquired using Centro XS3 LB 960 microplate luminometer (Berthold Technologies).

2.7. Statistical analysis

Data are presented as mean ± standard deviation (SD) from at least three independent experiments. Statistical analyses were performed using two-tailed Student's t-test.

3. Results

3.1. Chemistry

Using the commercially available substrate, 4 series of derivatives were designed and synthesized. The obtained compounds were further evaluated for their anti-RSV and anti-IAV activities.

The *N*-methyl-1H-indole analogues **6a-h**, **7a-c**, and **8d-f** were synthesized according to the route outlined in **Scheme 1.** This route started with the commercially-available 1-methyl-1H-indol. The key intermediate **5** was constructed in one pot using a method reported [29] with good yield (85%). Subsequently, it was coupled with different substitutive anilines to yield the *N*-methyl-1H-indole analogues **6a-h**. Initially, **6d** and **6f** were obtained in a yield of no more than 10% when the coupling reaction was conducted with 1-Ethyl-3-(3-Dimethylaminopropyl) Carbodiimide (EDC). Considering the low reactivity of aniline, a more efficient coupling reagent, Hexafluorophosphate Azabenzotriazole Tetramethyl Uronium (HATU), was used instead of EDC, and all target products **6a-h** were yielded in moderate to high yields (42.2% - 86.1%). At last, the analogues were oxidized to the corresponding sulfoxide and sulfone using different amounts of meta-chloroperoxybenzoic acid quantitatively.

The analogues, **14a-i** and 1**4'a-j**, were synthesized according the route outlined in **Scheme 2.** Compounds 3,4-di-chloroaniline **9** and 2-ethoxyaniline **10** were acylated with bromoacetyl bromide **11** to yield the 2-bromo-*N*-phenylacetamides **12** and **12'** (yield: 88.7% and 91.0% respectively). Subsequently, the 2-bromo-N-phenylacetamides were converted to the corresponding sodium sulfurothioates **13** and **13'**, which reacted with the substituted indoles to yield the target products **14a-h** and **14'a-i** by a nucleophilic attack in the presence of a catalytic amount of iodine (yield: 68.3% - 81.4% for 2 steps from compound **12**/**12'**). While preparing compound **14'b**, a byproduct **14'i** with an additional 7-bromination substitution was obtained (13.5%) with the target product. This byproduct was derived by bromination of 6-methoxyl indole or compound **14'b** by bromide ion generated in the previous steps in the presence of iodine. Compound **14'i** was also evaluated for its anti-viral activity and as one of the most potent compounds with both anti-RSV and anti-IAV activity. While preparing the azaindole analogues, the 7-azaindole analogues **14j** and **14'j** were obtained only in low yields of 8.4% and 6.7%, and the 4-, 5- and 6-aza-indole analogues could not be formed under this reaction condition. This can be explained by the oxidation of 1H-pyrrolo(2,3-c)pyridine, 1H-pyrrolo(3,2-c)pyridine, and 1H-pyrrolo(3,2-b)pyridine in the presence of iodine (**Scheme 3**), and the decreased nucleophilicity of the aromatic ring that caused a more difficult iodination. Although 1H-pyrrolo(2,3-b)pyridine can be oxidized under this condition, the intramolecular hydrogen bond between N and H-N obstructed the oxidation and hence

the same target product could be yielded.

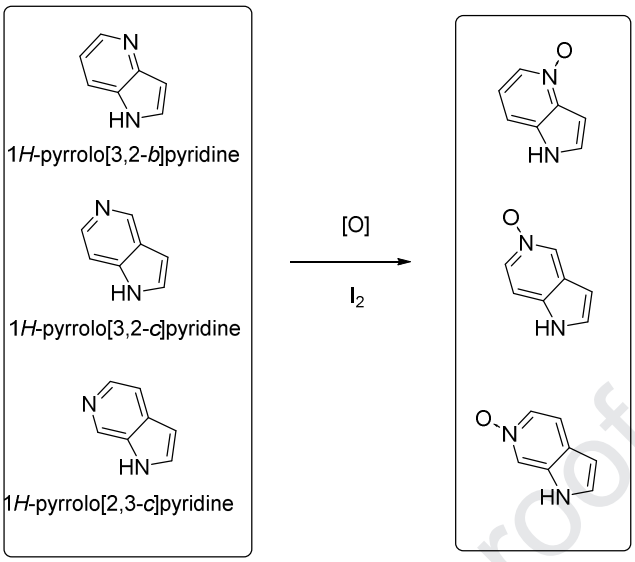

Scheme 3. Oxidation of the azaindole in the present of iodine.

3.2. Biological results

3.2.1. Evaluation of anti-RSV activity and cytotoxicity

After the synthesis of the target products, they were evaluated for their anti-RSV activity and cytotoxicity in an in vitro cell-based assay. Most of these derivatives possessed a potent anti-RSV profile compared to that of the reference compound, ribavirin (**Table 1**).

Compounds **6a-h** were derived from lead **1**. When an *N*-methyl was introduced to the indole ring, compound **6h** showed increased anti-RSV activity compared to that by lead **1** (EC_{50}=12.46±1.97 μM vs. EC_{50}=32.70±2.09 μM). Compounds **6d-6h** were di-chlorine substituted derivatives, of which, **6g** and **6h** exhibited good anti-RSV

activities with an EC_{50} value of 17.27±0.73 and 12.46±1.97 μM. The activity of these derivatives might be due to their symmetric substitution on the aromatic ring of phenylamine. Besides, **6d**, **6e**, and **6f** were not active with asymmetric substitution. Derivatives **6a-c** had one chlorine substituted on the phenylamine ring, of which, **6b** displayed similar activity to **6h** while **6c** was inactive. Such finding indicates that 3-Cl is more important than 4-Cl for anti-viral activity. The 2-Cl substituted **6a** was also inactive. Compound **6a** showed limited anti-RSV activity, but when oxidized to the corresponding sulfoxide **7a**, it possessed an anti-RSV activity with EC_{50} of 12.34±1.43 μM. For the comparison of the activity of thioether, sulfoxide **7a-c** and sulfone **8d-f** indicated that when the oxygen atom was introduced into the molecules, the orientation of phenylamine changed, ultimately altering the optimal position of chlorine substitution on phenylamine for anti-RSV activity. The preliminary structure-activity relationship revealed that the ability of a compound to inhibit RSV is mainly dependent on the number and position of the chlorine substituent on the phenylamine ring.

To explore the structure-activity relationship between the structure of indole ring and its anti-RSV activity, compounds **14a-h, 14j**, and **14'a-j** were designed and synthesized. Most of the compounds with a mono-chlorine or methoxy group (i.e., **14b**, **14g, 14'a, 14'c, 14'e**, **14'f**, and **14'h**) on the indole ring depicted excellent to moderate activity. Compound **14'a**, with a 7-MeO on the indole ring, had the most potent anti-RSV activity (EC_{50}=0.43±0.10 μM), a value indicating 27-fold more

potent activity than the lead **2** and 76-fold greater activity than lead **1**. With an increase in anti-viral activity, toxicity of the mono-chlorine or methoxy substituted derivatives decreased (i.e., **14b**, **14'c**, **14'd**, **14'e**, and **15'g**). Compound **14'c** was identified as the most promising lead with a safety index (SI= CC_{50}/ EC_{50}) of 379.25. When another nitrogen-atom was introduced onto the indole ring, the compounds became inactive (**14j** vs. **1** and **14'j** vs. **2**).

Most of the compounds in series **14** and **14'** were more potent than those in series **6-8.** The EC_{50} values of the most potent compounds **14b, 14'a, 14'c, 14'e, 14'f, 14'h,** and **14'i** for RSV inhibition effect were 5.79±1.20, 0.43±0.10, 4.82±0.99, 4.46±0.28, 5.58±0.02, 2.45±0.40, and 2.92±0.77 μM, respectively. All compounds showed a dose-dependent inhibition to RSV. Dose-response curve is shown in **Figure 4**.

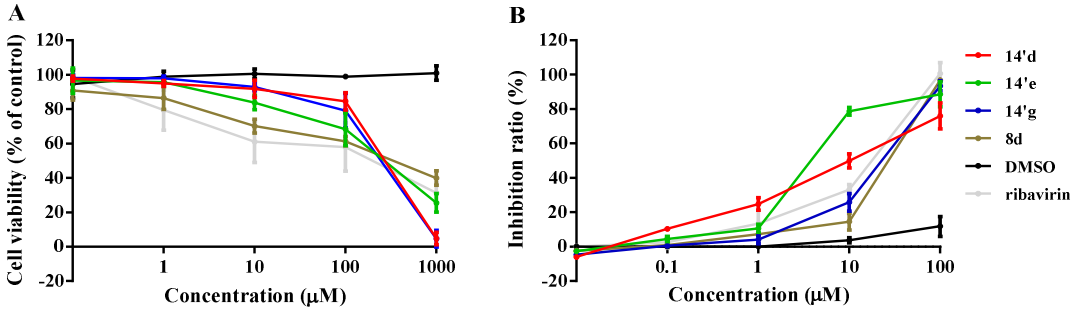

Figure 4 Dose-response curve for compounds **8d, 14'd, 14'e, 14'g** on HEp-2 cell viability and RSV inhibition. The compounds tested were dissolved in DMSO as a solution of 100mM and diluted to the concentration indicated. The concentration of DMSO (v/v) used to determine the cells activity was 0.01‰, 0.1‰, 1‰, and 10‰, respectively; and the concentration of DMSO used to determine the inhibition rate

was 0.001‰, 0.01‰, 0.1‰ and 1‰, respectively. Data are representative of three independent experiments and values are expressed as mean ± SD.

To derive the stage of virus replication where these compounds exerted their antiviral activity, the most promising compound **14'c** was added before or after RSV infection. As shown in **Figure 5**, pretreatment was unnecessary for full (99.94% and 99.89%) antiviral activity. Treatment at times -1 h and 0 h with 20 μM of **14'c** resulted in similar and full virus inhibition effects. This result suggests that compound **14'c** inhibits RSV replication at post viral entry.

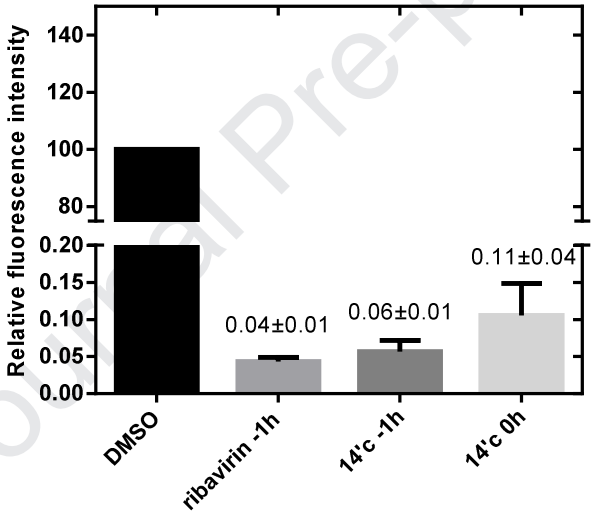

Figure 5 Anti-RSV effect of **14'c** with and without pretreatment. Compound **14'c** (20 μM) was added to the culture medium before infection (-1 h) or after infection (0 h). DMSO and ribavirin were used as negative and positive controls, respectively. The level of RSV-mGFP infection was determined by measuring fluorescence levels. Data are normalized to control group, with the value of control arbitrarily set as 1. Data are representative of three independent experiments and values are expressed as mean ± SD.

3.2.1. Evaluation of anti-IAV activity

We proceeded to assess the anti-IAV effect of these compounds and found that the most potent compounds **6g**, **6h**, **14'c**, **14'f**, and **14'i** displayed inhibition greater than 85% against IAV A/WSN/33 (H1N1) at a concentration of 10 μM (data not shown). This inspiring result encouraged us to further evaluate their anti-IAV effect at different concentrations. Most of these compounds depicted moderate to excellent activity (**Table 2**). Compounds **6g**, **6h**, **14'c**, **14'e**, **14'f**, **14'h**, and **14'i** were identified as the most potent IAV inhibitors with low micromolar to sub-micromolar EC_{50} values.

Compounds **6a-h**, **7a-c**, and **8d-f** with a common N-Methyl substitution on the indole ring showed relatively low activity and cytotoxicity unlike **14a-h** and **14'a-i**. This result indicates that the substitution of the N-hydrogen on the indole ring may reduce the toxicity of these IAV inhibitors. Compounds **14a-h** and **14j** have a common 3,4-di-Cl substitution on the aniline. When a methoxy group was introduced into these molecules on the benzene ring in indole, compounds **14a-d** displayed similar antiviral effects with EC_{50} values in the 15-μM range. Such finding indicates that the position of the methoxy group is not crucial. Higher activity was observed for derivatives **14e-h** bearing the same chlorine atom on different positions of the benzene ring in indole. When another nitrogen atom was introduced onto the indole ring, compound **14j** showed decreased activity with an EC_{50} value of 32 μM. Compounds **14'a-j** had a common 2-ethoxyl substitution on the aniline and showed relatively higher inhibitory

effect than the corresponding **14a-h** and **14j.** This result demonstrates that a 2-ethoxyl substitution on the aniline is superior to a 3,4-di-Cl substitution for the anti IAV effect. The increased IAV inhibitory effect of compounds **14e-f** compared to that of **14a-d** also demonstrate a chlorine atom substitution on different position of the benzene ring in indole is crucial for their anti IAV effect.

Results obtained suggest that *N*-hydrogen on the indole ring may be related to its cytotoxicity. All compounds with a 2-ethoxyl substitution on the aniline and a chlorine/bromine substitution on the indole ring pose a high IAV inhibitory effect.

All compounds showed dose-dependent anti-IAV effect. The representative dose-response curve for the most potent compounds **6g**, **14'c**, **14'f**, **14'h** and **14'i** are shown in **Figure 6** and the EC_{50} values were 0.64, 1.26, 1.53, 0.60, and 1.90 μM, respectively.

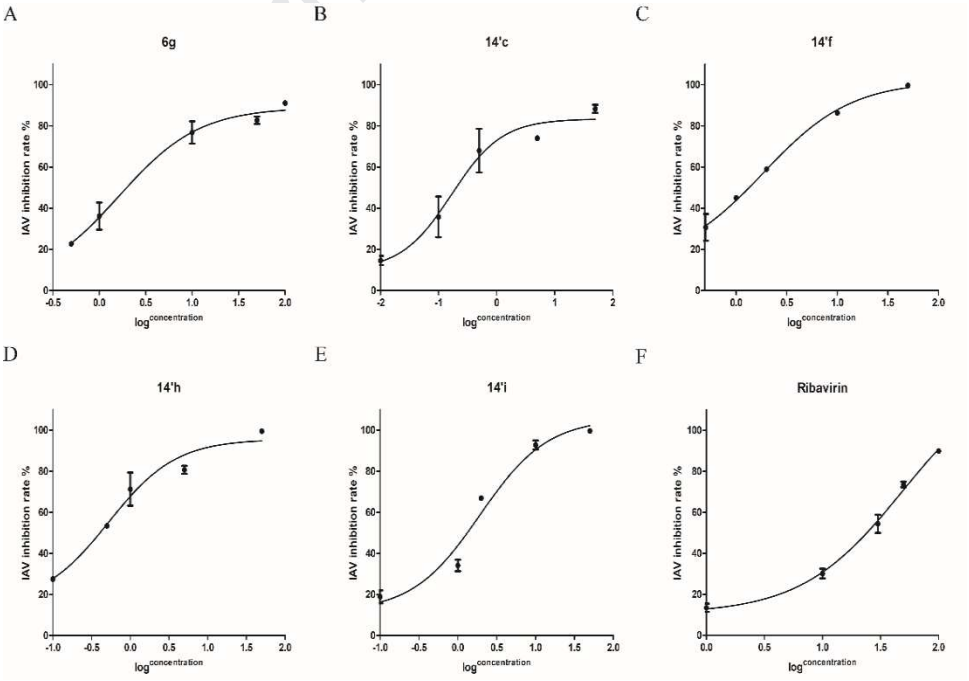

Figure 6 Dose-response curve for compounds **6g**, **14'c**, **14'f**, **14'h**, **and 14'i**. The serially-diluted concentrations of test compounds were added to the culture medium.

Ribavirin was used as the positive control. The level of IAV A/WSN/33 (H1N1) infection was determined by measuring Gluc activity. Data are normalized to control group, with the value of control arbitrarily set as 100%. Data are representative of three independent experiments and values are expressed as mean ± SD.

Compounds **6g**, **14'e**, **14'f**, **14'h**, and **14'i** were selected to evaluate their antiviral effect in MDCK cells against H1N1 and H3N2, which are important causes of human influenza. All of these compounds showed a more potent inhibitory effect than ribavirin against both of these two IAVs. (**Figure 7**). The EC_{50} values of compounds **6g**, **14'e**, **14'f**, **14'h**, and **14'i** against H1N1 were 1.75, 4.33, 2.42, 2.67, and 3.25μM, and that against H3N2 were 1.50, 1.83, 1.58, 2.33, and 1.50μM, while the EC_{50} values of ribavirin against both virus were measured as 16.0 and 20.5μM, respectively.

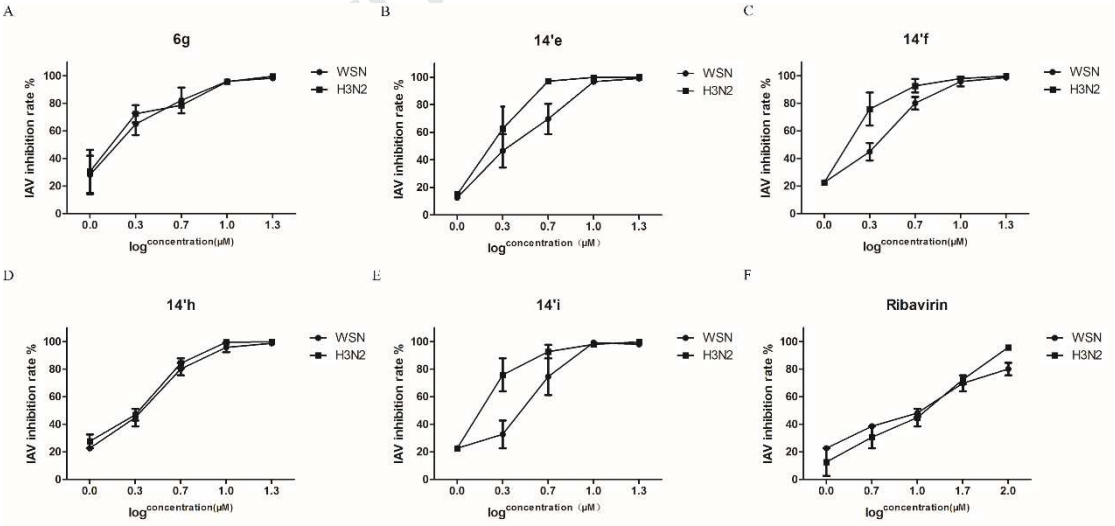

Figure 7 Antiviral effect of compounds **6g**, **14'e**, **14'f**, **14'h**, **and 14'i** against H1N1 and H3N2 in MDCK cells. The serially-diluted concentrations of test compounds were added to the culture medium. Ribavirin was used as the positive control. The level of IAV A/WSN/33 (H1N1) and H3N2 infection was determined by measuring

Gluc activity. Data are normalized to control group, with the value of control arbitrarily set as 100%. Data are representative of three independent experiments and values are expressed as mean ± SD.

Notably, the most potent anti-IAV compounds **6g**, **6h**, **14'c**, **14'e**, **14'f** , **14'h**, and **14'i** showed potency in the anti-RSV assay above, and **14'c**, **14'e**, **14'f**, **14'h**, and **14'i** exhibited excellent activity against both RSV and IAV. Such finding suggests that these compounds may employ a similar mechanism to control the replication of both viruses. In support of this notion, we observed that compounds **14'f** and **14'i** inhibited IAV replication at the post-entry stage, similar to that found for RSV. For instance, treatment before or after IAV infection (at time -2 h and 0 h) with 20 μM of **14'i** or **14'f** resulting in similar and complete inhibitory effects on IAV replication (99.72%-99.86%, see **Figure 8**).

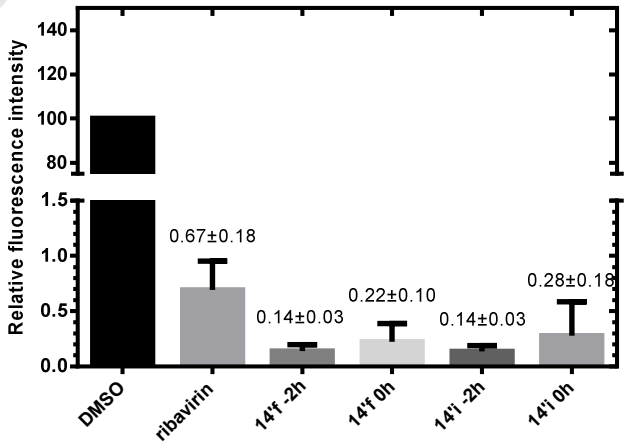

Figure 8 Time of addition assay of **14'f** and **14'i**. Test compounds (20 μM) were added to the culture medium before infection (-1 h) or during infection (0 h). DMSO and ribavirin were used as negative and positive controls, respectively. The level of

IAV A/WSN/33 (H1N1) infection was determined by measuring Gluc activity. Data are normalized to control group, with the value of control arbitrarily set as 100%. Data are representative of three independent experiments and values are expressed as mean ± SD.

To further explore the action of these active compounds, we investigated their effect on IAV RNA transcription and replication using an IAV mini-genome replicon system. IAV polymerase activity was reconstituted by expressing A/WSN/33 (H1N1) RdRp subunits (PA, PB1 and PB2), NP, and a vRNA-like reporter gene Gluc (PolI-luc) in 293T cells as described previously [30]. The result showed that compounds **14'i** and **14'f** significantly inhibited the activity of luciferase in a dose-dependent manner, with EC_{50} values of 1.98 μM and 3.89 μM, respectively (**Figure 9**). The similar potency of compounds **14'i** and **14'f** for the inhibition of IAV infectivity and RdRp activity suggests that these compounds may target viral RNA transcription and replication.

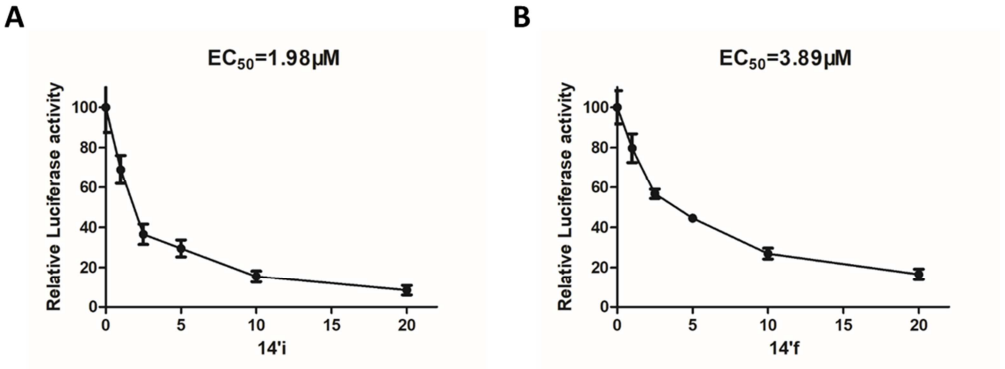

Figure 9 Effect of compounds **14'i** and **14'f** on IAV vRNP. HEK239T cells were co-transfected with pCAGGS expression plasmids encoding PB2, PB1, PA, NP, and PolI-LUC in the absence or presence of compound **14'i** or **14'f** (1 μM, 2.5 μM, 5 μM, 10 μM, or 20 μM). At 24 h post-transfection, effects of vRNA transcription was determined by measuring luciferase activity. Data are normalized to control group,

with the value of control arbitrarily set as 100%. Data are representative of three independent experiments and values are expressed as mean ± SD.

4. Conclusions

RSV and IAV cause substantial morbidity and mortality, and mainly affect infants and elderly persons worldwide. In this study, the anti-viral potential of a series of 2-((1H-indol-3-yl)thio)-N-phenyl-acetamide was revealed. The developed compounds displayed moderate to high activity against both viruses, with compounds **14'c**, **14'e**, **14'f**, **14'h**, and **14'i** exhibiting excellent activity at low micromolar to sub-micromolar EC_{50} values. Among these compounds, **14'c** and **14'e**, and **14'f** and **14'i** were identified as the most promising dual inhibitors, displaying lower cytotoxicity (with highest safety index up to 379.25) than the clinical drug, ribavirin. The preliminary results imply that these 2-((1H-indol-3-yl)thio)-N-phenyl-acetamide derivatives exert their antiviral activity at the viral post-entry stage. Such findings can significantly contribute to the discovery of novel and potent drugs against respiratory syncytial virus and influenza A infection, thereby providing great protection for individuals at both ends of the age spectrum.

Declarations of interest: None

Acknowledgments

The research was supported by the National Natural Science Foundation of China

(grant number 81703366 ZGN), The National Mega-Project for drug renovation (grant numbers 2018ZX09711003-002-002 ZJM, 2019ZX09201001-003-007 WYC), CAMS innovation fund for Medical Sciences (grant numbers 2016-I2M-1-011 WYC, 2016-I2M-3-014 WJX, 2017-I2M-3-019 BXG, and 2018-I2M-3-004 WJ), the Fundamental Research Funds for the Central Universities (grant number 332017078 ZGN), and Fundamental Research Funds for Jinzhou Medical University (grant number JYTQN201731 LZQ).

References

[1]. Liu, L., Oza, S., Hogan, D., et al., 2015. Global, regional, and national causes of child mortality in 2000–13, with projections to inform post-2015 priorities: an updated systematic analysis. Lancet 385, 430-440.

[2]. Jain, S., Williams, D.J., Arnold, S.R., et al., 2015. Community-acquired pneumonia requiring hospitalization among U.S. children. N. Engl. J. Med. 372, 835-845.

[3]. Jain, S., Self, W.H., Wunderink, R.G., et al., 2015. Community-acquired pneumonia requiring hospitalization among U.S. adults. N. Engl. J. Med. 373, 415-427.

[4]. Bhuyan, G. S., Hossain, M. A., Sarker, S. K., et al., 2017. Bacterial and viral pathogen spectra of acute respiratory infections in under-5 children in hospital settings in Dhaka city. PLoS ONE 12, e0174488.

[5]. Hardy, R. W., Wertz, G. W., 2000. The Cys3-His1 motif of the respiratory syncytial virus M2-1 protein is essential for protein function. J. Virol. 13, 5880-5885.

[6]. Thompson, W. W., Shay, D. K., Weintraub, E., et al., 2003. Mortality associated with

influenza and respiratory syncytial virus in the United States. J. Am. Med. Assoc. 289, 179-186.

[7]. Elliot, A. J., Fleming, D. M., 2008. Influenza and respiratory syncytial virus in the elderly. Expert Rev. Vaccines 7, 249-258.

[8]. Nair, H., Nokes, D. J., Gessner, B. D., et al., 2010. Global burden of acute lower respiratory infections due to respiratory syncytial virus in young children: a systematic review and meta-analysis. Lancet 375, 1545-1555.

[9]. Blanken, M. O., Rovers, M. M., Molenaar, J. M., et al., 2013. Respiratory syncytial virus and recurrent wheeze in healthy preterm infants. N. Engl. J. Med. 368, 1791-1799.

[10]. Palomo, C., Mas, V., Detalle, L., et al., 2016. Trivalency of a nanobody specific for the human respiratory syncytial virus fusion glycoprotein drastically enhances virus neutralization and impacts on escape mutant selection. Antimicrob. Agents Ch. AAC-00842.

[11]. Cancellieri, M., Bassetto, M., Widjaja, I., et al., 2015. In silico structure-based design and synthesis of novel anti-RSV compounds. Antivir. Res. 122, 46-50.

[12]. Patel, K., Kirkpatrick, C. M., Nieforth, K. A., et al., 2019. Respiratory syncytial virus-A dynamics and the effects of lumicitabine, a nucleoside viral replication inhibitor, in experimentally infected humans. J. Antimicrob. Chemother. 2018, dky415.

[13]. Hanfelt-Goade D., Maimon N., Nimer A., et al., 2018. A Phase 2b, randomized, double-blind, placebo-controlled trial of presatovir (GS-5806), a Novel Oral RSV fusion inhibitor, for the treatment of respiratory syncytial virus (RSV) in hospitalized adults//C17. New Insights in Acute Pulmonary Infections. Am. Thorac. Soc. 2018: A4457

[14]. Brookes, D. W., Coates M, Allen H, et al., 2018. Late therapeutic intervention with a

respiratory syncytial virus L-protein polymerase inhibitor, PC786, on respiratory syncytial virus infection in human airway epithelium. Br. J. Pharmacol. 175, 2520-2534.

[15]. Israel S., Rusch S., DeVincenzo J., et al., 2016. Effect of oral JNJ-53718678 (JNJ-678) on disease severity in healthy adult volunteers experimentally inoculated with live respiratory syncytial virus (RSV): a placebo-controlled challenge study//Oh, Those Pesky Viruses! 2016. https://idsa.confex.com/idsa/2016/webprogram/Paper59339.html.

[16]. Ark Biosciences, 2017. A study of AK0529 to evaluate pharmacokinetics and safety in Chinese healthy volunteers. ClinTrials.gov, NCT03322800.

[17]. Cockerill, G. S., Good, J. A., Mathews, N., 2019. State of the Art in Respiratory Syncytial Virus Drug Discovery and Development. J. Med. Chem. 62, 3206-3227.

[18]. El Saleeby, C. M., Bush, A. J., Harrison, L. M., et al., 2011. Respiratory syncytial virus load, viral dynamics, and disease severity in previously healthy naturally infected children. J. Infect. Dis. 204, 996-1002.

[19]. Iuliano, A. D., Roguski, K. M., Chang, H. H., et al., 2018. Estimates of global seasonal influenza-associated respiratory mortality: a modelling study. Lancet 391, 1285-1300.

[20]. Zhou, H., Thompson, W. W., Belongia, E. A., et al., 2018. Estimated rates of influenza‐associated outpatient visits during 2001‐2010 in 6 US integrated healthcare delivery organizations. Influenza Other Resp. 12, 122-131.

[21]. Jannetto, P. J., Buchan, B. W., Vaughan, K. A., et al., 2010. Real-time detection of influenza A, influenza B, and respiratory syncytial virus A and B in respiratory specimens by use of nanoparticle probes. J. Clin. Microbiol. 48, 3997-4002.

[22]. Shen, Z., Lou, K., Wang, W., 2015. New small-molecule drug design strategies for fighting

resistant influenza A. Acta Pharm. Sin. B. 5, 419-430.

[23]. Deyde, V. M., Xu, X., Bright, R. A., et al., 2007. Surveillance of resistance to adamantanes among influenza A(H3N2) and A(H1N1) viruses isolated worldwide. J. Infect. Dis. 196, 249-257.

[24]. Sheu T.G., Deyde V.M., Okomo-Adhiambo M., et al., 2008. Surveillance for neuraminidase inhibitor resistance among human influenza A and B viruses circulating worldwide from 2004 to 2008. Antimicrob. Agents Chemother. 52, 3284–3292.

[25]. Crowther, Z., 2012. Influenza and RSV: know the diagnostic options. MLO: Med. Lab. Obs. 44, 36.

[26]. Gonzàlez-Parra, G., De Ridder, F., Huntjens, D., et al., 2018. A comparison of RSV and influenza in vitro kinetic parameters reveals differences in infecting time. PloS ONE 13, e0192645.

[27]. Gao, Q., Wang, Z., Liu, Z., et al., 2014. A cell-based high-throughput approach to identify inhibitors of influenza A virus. Acta. Pharm. Sin. B. 4, 301-306.

[28]. Tannous, B. A., 2009. Gaussia luciferase reporter assay for monitoring biological processes in culture and in vivo. Nat. Protoc. 4, 582-591.

[29]. Mirskova, A. N., Levkovskaya, G. G., Kolesnikova, O. P., et al., 2010. Directed synthesis and immunoactive properties of (2-hydroxyethyl) ammonium salts of 1-R-indol-3-ylsulfanyl (sulfonyl) alkanecarboxylic acids. Russ. Chem. Bull. 59, 2236-2246.

[30]. Wang, J., Wang, Y., Zhou, R., et al., 2018. Viruses 10, 330.

Table 1 Structure, anti-RSV activity, and cytotoxicity of the target products.

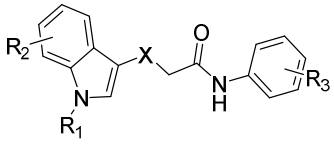

1, 2, 6, 7, 8, 14 and 14'

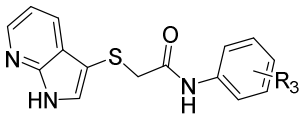

14j and 14'j

Compd	Structure				EC_{50} (μM)*	CC_{50} (μM)*	Safety Index SI= CC_{50}/ EC_{50}
	R_1	R_2	X	R_3			
1	H	H	S	3,4-di-Cl	32.70±2.09	37.48±1.78	1.15
2	H	H	S	2-EtO	11.76±3.36	20.74±5.75	1.76
6a	Me	H	S	2-Cl	>128	>1000	-[b]
6b	Me	H	S	3-Cl	23.92±3.48	18.93±0.93	0.79
6c	Me	H	S	4-Cl	>128	31.39	-[a]
6d	Me	H	S	2,3-di-Cl	>128	>1000	-[a]
6e	Me	H	S	2,4-di-Cl	>128	>1000	-[a]
6f	Me	H	S	2,5-di-Cl	>128	76.89	-[a]
6g	Me	H	S	2,6-di-Cl	17.27±0.73	23.65±1.55	1.37
6h	Me	H	S	3,4-di-Cl	12.46±1.97	30.51±9.62	2.45
7a	Me	H	S=O	2-Cl	12.34±1.43	97.42±3.48	7.89
7b	Me	H	S=O	3-Cl	>128	>1000	-[a]
7c	Me	H	S=O	4-Cl	>128	61.88	-[a]
8d	Me	H		2,3-di-Cl	19.94±5.43	275.05±28.85	13.79
8e	Me	H		2,4-di-Cl	>128	>1000	-[a]
8f	Me	H		2,5-di-Cl	>128	>1000	-[a]
14a	H	7-MeO	S	3,4-di-Cl	17.28±1.44	39.47±2.66	2.28
14b	**H**	**6-MeO**	**S**	**3,4-di-Cl**	**5.79±1.20**	**42.67±4.70**	**7.16**
14c	H	5-MeO	S	3,4-di-Cl	16.59±1.90	46.35±0.735	2.79
14d	H	4-MeO	S	3,4-di-Cl	>128	>256	-[a]
14e	H	7-Cl	S	3,4-di-Cl	18.12±0.72	32.83±0.73	1.81
14f	H	6-Cl	S	3,4-di-Cl	13.95±0.02	27.79±1.86	1.99
14g	H	5-Cl	S	3,4-di-Cl	9.95±0.28	35.20±2.04	3.54
14h	H	4-Cl	S	3,4-di-Cl	25.34±1.17	27.74±2.91	1.09
14j	-[a]	-[a]	-[a]	3,4-di-Cl	>128	>256	-[a]
14'a	H	7-MeO	S	2-EtO	0.43±0.10	0.61±0.05	1.42
14'b	H	6-Me	S	2-EtO	23.07±6.01	35.23±4.34	1.53

14'c	**H**	**5-MeO**	**S**	**2-EtO**	**4.82±0.99**	**1828.00±84.00**	**379.25**
14'd	H	4-MeO	S	2-EtO	12.28±1.32	220.35±12.25	17.94
14'e	**H**	**7-Cl**	**S**	**2-EtO**	**4.46±0.28**	**262.30±24.90**	**58.81**
14'f	**H**	**6-Cl**	**S**	2-EtO	5.58±0.02	29.95±0.39	5.36
14'g	H	5-Cl	S	2-EtO	18.13±2.75	204.45±0.05	11.27
14'h	**H**	**4-Cl**	**S**	2-EtO	2.45±0.40	7.15±0.02	2.92
14'i	**H**	**6-MeO**	**S**	2-EtO	2.92±0.77	9.65±0.88	3.30
14'j	- [a]	- [a]	- [a]	2-EtO	>128	>1000	- [a]
Ribavirin	- [a]	- [a]	- [a]	- [a]	15.83±3.38	273.80±4.13	17.30

*Data are expressed as Mean±SD of three independent experiments, test of **CC_{50}** values was not repeated for inactive compounds; - [a]: not applicable.

Table 2 Structure, anti-IAV activity and cytotoxicity of the target products

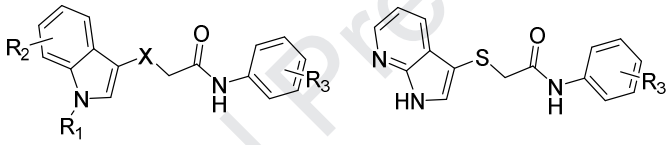

6, 7, 8, 14 and 14' 14j and 14'j

Compd	Structure				EC_{50}(μM)	CC_{50}(μM）	Safety Index
	R1	R2	X	R3			**SI= CC_{50}/ EC_{50}**
6a	Me	H	S	2-Cl	27.94±3.89	>100	>3.59
6b	Me	H	S	3-Cl	9.98±0.36	>100	>10.02
6c	Me	H	S	4-Cl	9.82±1.54	>100	>10.17
6d	Me	H	S	2,3-di-Cl	13.96±2.22	>100	>7.26
6e	Me	H	S	2,4-di-Cl	11.93±0.24	>100	>8.38
6f	Me	H	S	2,5-di-Cl	15.75±2.02	>100	>6.38
6g	Me	H	S	2,6-di-Cl	3.50±0.48	>100	>28.57
6h	Me	H	S	3,4-di-Cl	0.64±0.02	>100	>156.25
7a	Me	H	S=O	2-Cl	29.78±1.04	>100	>3.36
7b	Me	H	S=O	3-Cl	39.27±2.70	>100	>2.55
7c	Me	H	S=O	4-Cl	9.93±0.39	>100	>10.00
8d	Me	H		2,3-di-Cl	36.34±0.18	>100	>2.75
8e	Me	H		2,4-di-Cl	33.71±0.48	>100	>2.97
8f	Me	H		2,5-di-Cl	18.03±7.30	>100	>6.72
14a	H	7-MeO	S	3,4-di-Cl	13.81±0.81	>100	>7.21
14b	H	6-MeO	S	3,4-di-Cl	15.80±3.21	78.44±2.10	5.00

14c	H	5-MeO	S	3,4-di-Cl	15.45±5.57	61.75±6.31	4.19
14d	H	4-MeO	S	3,4-di-Cl	15.08±0.63	>100	>6.61
14e	H	7-Cl	S	3,4-di-Cl	10.41±0.63	49.07±2.70	4.69
14f	H	6-Cl	S	3,4-di-Cl	7.36±1.06	67.79±2.63	9.16
14g	H	5-Cl	S	3,4-di-Cl	7.62±1.57	42.66±1.36	5.53
14h	H	4-Cl	S	3,4-di-Cl	5.72±1.48	34.70±0.92	5.95
14j	- [a]	- [a]	- [a]	3,4-di- [a]l	31.56±4.84	>100	>3.10
14'a	H	7-MeO	S	2-EtO	12.20±2.00	>100	>8.24
14'b	H	6-MeO	S	2-EtO	4.48±0.22	88.20±1.09	15.36
14'c	**H**	**5-MeO**	**S**	**2-EtO**	1.27±0.07	>100	**>79.37**
14'd	H	4-MeO	S	2-EtO	11.21±3.04	>100	8.80
14'e	**H**	**7-Cl**	**S**	**2-EtO**	1.75±0.96	>100	**>57.47**
14'f	**H**	**6-Cl**	**S**	**2-EtO**	1.53±0.39	>100	**>65.36**
14'g	H	5-Cl	S	2-EtO	4.19±0.73	37.62±2.90	8.97
14'h	**H**	**4-Cl**	**S**	**2-EtO**	0.58±0.22	25.23±4.07	**>40.97**
14'i	**H**	**6-MeO 7-Br**	**S**	**2-EtO**	1.90±0.05	>100	**>52.63**
14'j	- [a]	- [a]	- [a]	2-EtO	31.42±2.68	>100	3.21
ribavin	- [a]	- [a]	- [a]	- [a]	25.08±2.28	>100	>3.99

* Data are expressed as Mean±SD of three independent experiments; - [a]: not applicable.

Highlights

- RSV and IAV cause substantial morbidity and mortality
- The developed compounds displayed moderate to high activity against both viruses
- **14'c**, **14'e**, **14'f**, **14'h** and **14'I** had excellent activity at low to sub-micromolar EC_{50}
- **14'c** and **14'e**, and **14'f** and **14'i** were the most promising dual inhibitors
- The derivatives exert their antiviral activity at the viral post-entry stage